Optik 165 (2018) 370–379

Contents lists available at ScienceDirect

Optik

journal homepage: www.elsevier.de/ijleo

Original research article

Electronic structure, optical and structural properties of organic 5,5′-Dibromo-2,2′-bithiophene

Mustafa Kurban [a], Bayram Gündüz [b,*]

[a] Department of Electronics and Automation, Ahi Evran University, 40100 Kırşehir, Turkey
[b] Department of Science Education, Faculty of Education, Muş Alparslan University, 49250 Muş, Turkey

ARTICLE INFO

Article history:
Received 28 February 2018
Accepted 1 April 2018

Keywords:
Organic molecules
UV–vis spectroscopy
Electronic structure
Refractive index
DFT

ABSTRACT

The changes in the electronic, optical and structural properties of the title compound have been investigated using experimental and theoretical techniques. The semi-emprical relations have been proposed for the calculation of the refractive index (n) from its measured and calculated energy gap (E_g) data. The simulated IR and Raman spectra characteristics and HOMO-LUMO energies, harmonic frequencies, Mulliken atomic charges, radial distribution functions (RDFs) and coordination number of binary interactions were recorded with the aid of density functional theory (DFT) based on optimized structure for different solvent environments. Ultraviolet-visible (UV–vis) spectral analysis has been carried out using experimental techniques and time-dependent (TD) DFT calculations. Furthermore, the effects of the concentrations on the optoelectronic properties were experimentally investigated. The measured and calculated results are discussed to get an insight for the future optoelectronic applications.

1. Introduction

Recently, organic semiconductors have attracted great attention as potential advanced materials used in many electronic, optoelectronic, and photonic applications [1] such as solar cells [2–5] photovoltaics [4,5] light emitting diodes [4,6] sensors [7,8], chemical sensors [9], vapour sensors [10], gas sensors [11,12] and photodetectors [13]. Among the semiconductors, small molecule semiconductor materials in combination with polymer binders and suitable solvents are the most widely used in areas including the field of organic electronic applications [14,15] because they potentially provide high-quality chain alignment and can be reliably synthesized with accurate molecular weight control without significant batch-to-batch variations [16,17].

5,5′-Dibromo-2,2′-bithiophene organic molecule is a key intermediate of a variety of oligothiophene derivatives, which are widely applied as advanced organic materials [18–20]. For example, the related reactions of 5,5′-Dibromo-2,2′-bithiophene with 2-tri-*n*-butylstannyl-5-*n*-hexylpyridine with the use of this co-catalyst produced the desired materials in 44% purified yields [21]. Organic two-photon absorption chromophores were designed and synthesized using the 5,5′-Dibromo-2,2′-bithiophene and found suitable for biological applications in live specimens [22]. 5,5′-Dibromo-2,2′-bithiophene-based the polymers was also found to increase the performance of organic field-effect transistors [23], and

* Corresponding author.
E-mail addresses: mkurbanphys@gmail.com, mkurban@ahievran.edu.tr (M. Kurban), bgunduz@hotmail.com, b.gunduz@alparslan.edu.tr (B. Gündüz).

https://doi.org/10.1016/j.ijleo.2018.04.003
0030-4026/

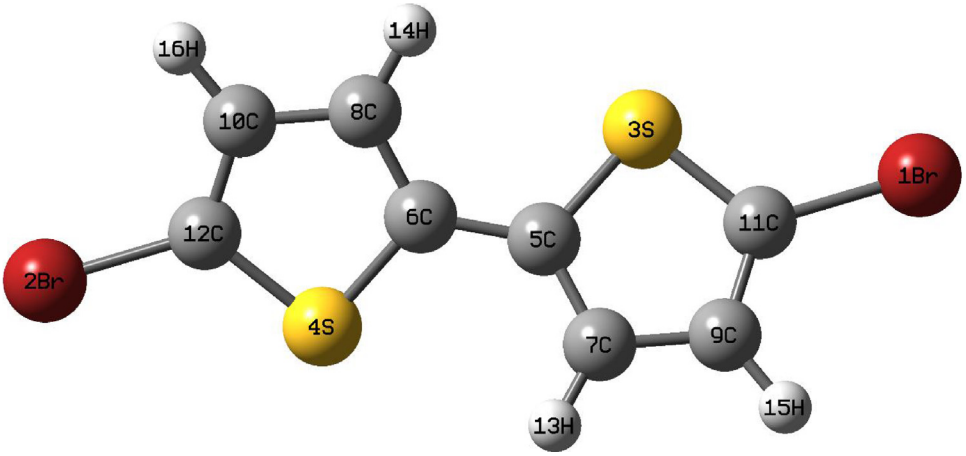

Fig. 1. Optimized ground state geometry with atom numbering calculated by B3LYP/6-311-G (d, p). (For interpretation of the references to colour in this figure legend, the reader is referred to the web version of this article.)

organic photovoltaics [24]. In addition, the synthesized 5-(carbazol-9-yl)-5′-mercapto-2,2′-bithiophene based on 5,5′-Dibromo-2,2′-bithiophene demonstrated enhanced emission when it is attached to the surface of CdSe quantum dot [25].

To date there have been no studies about the structural, electronic, spectroscopic and optical properties of the title compound. The structural, electronic vibrational, optical properties of the related material were investigated in detail for different concentrations and solvents in this study. In this regard, we have analysed the optimized bond distances, angles, vibrational harmonic frequencies, process of geometry optimization, recractive index (n), simulated IR and Raman spectra characteristics, radial distribution functions (RDFs) and probability distributions in terms of coordination number of the binary interactions, the highest occupied molecular orbital (HOMO), the lowest unoccupied molecular orbital (LUMO) and the frontier molecular orbital energy gap (HOMO–LUMO difference in energy gap, E_g), Mulliken atomic charges of the small molecule using density functional theory (DFT) calculations. Using time-dependent (TD)-DFT method, the theoretically predicted the ultraviolet-visible (UV–vis), HOMO, LUMO and E_g of the small molecule have been compared with the measured results.

Later, the effects of the concentrations on the optical refractive index, $(\alpha h\vartheta)^2$ curves based on photon energy (E), The transmittance (T) and $dT/d\lambda$ based on λ, the mass extinction coefficient (α_{mass}) were experimentally investigated. Finally, measured and calculated these parameters based on different solvents and concentrations are discussed for optoelectronic applications in detail.

2. Experimental details

Solution technique has been used for the title organic compound to investigate spectroscopic, electronic and optical properties. The compund is provided from Sigma-Aldrich Chemical Company (USA) with a stated purity of 99% (HPLC). The solutions of the compound have been prepared for 0.68, 1.41 and 2.30 μM and then the weighed materials of the compound were dissolved homogeneously in 13 mL volume of chloroform solvent.

3. Computational details

The structural, electronic and spectroscopic properties of the title organic compound have been investigated using DFT [26] at the B3LYP level [27–29]. The 6–311 G (d, p) basis set has been used in the calculations. The calculations have been performed using the GAUSSIAN09 program package [30]. Various spin multiplicities were investigated and it has been found that the compound have spin singlet as the most stable (minimum total energy). The geometry of the compound was optimised without imposing any symmetrical constraints and the lowest total energy configuration was assumed as the global minimum case. The structure is taken as the local minima on potential energy surface having positive vibration frequencies. After geometric optimization, TD-DFT method used to get maximum wavelengths and compared with the experimental UV absorption and E_g of the compound.

4. Results and discussion

4.1. Structural analysis

Optimized ground state structure of the compound with atom numbering calculated by B3LYP/6-311-G (d, p) is shown in Fig. 1 and the corresponding bond distances obtained from gas phase, chloroform solvent and available measured data

Table 1
The bond distances (Å) of binary interactions in 5,5′-Dibromo-2,2′-bithiophene organic molecule for gas phase and chloroform solvent, together with measured results.

Interactions	Bond distances			Interactions	Bond distances	
	Gas phase	Chloroform	[a]Exp.		Gas phase	Chloroform
Br1—C11	1.8886	1.8905	1.869	C7—C9	1.4219	1.4224
Br2—C12	1.8886	1.8905	–	C7—H13	1.0819	1.0818
S3—C5	1.7569	1.7579	1.744	C8—C10	1.4219	1.4224
S3—C11	1.7380	1.7389	1.713	C8—H14	1.0819	1.0818
S4—C6	1.7570	1.7579	–	C9—C11	1.3642	1.3642
S4—C12	1.7380	1.7389	–	C9—H15	1.0808	1.0808
C5—C6	1.4514	1.4518	1.447	C10—C12	1.3642	1.3642
C5—C7	1.3733	1.3737	1.363	C10—H16	1.0808	1.0808
C6—C8	1.3733	1.3737	–			

[a] [31].

Table 2
Calculated first three vibrational harmonic frequencies (ω, in cm^{-1}) and the corresponding non-zero infrared intensities (in km/mol) (given in parenthesis) of 5,5′-Dibromo-2,2′-bithiophene organic molecule for different solvent environment.

Solvents	ω (Infrared intensities)		
Chloroform	34.70(0.1291)	44.31(0.5677)	51.95(0.0006)
Chlorobenzene	34.69(0.1359)	44.29(0.5810)	51.74(0.0005)
Dichloromethane	34.57(0.1505)	44.25(0.6060)	51.24(0.0001)

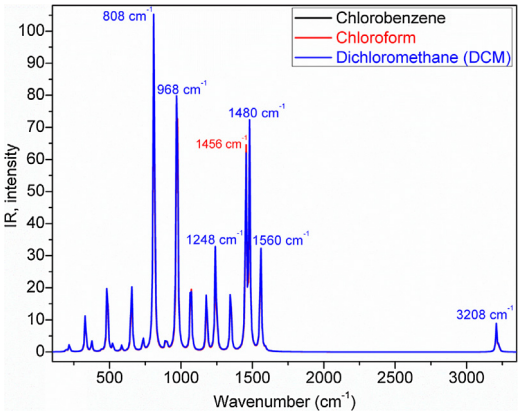

Fig. 2. Simulated IR spectra for different solvents. (For interpretation of the references to colour in this figure legend, the reader is referred to the web version of this article.)

are tabulated in Table 1. From the results, the bond distances increase from gas phase to solvation phase for Br-C, C—C and S—C interactions, however; C–H interactions are almost the same. The measure bond distances of Br1—C11, S3—C5, S3—C11, C5—C6 and C5—C7 are found to be 1.869 Å, 1.744 Å, 1.713 Å, 1.447 Å and 1.363 Å [31], respectively. Similarly, the bond angle of Br1—C11—S3, Br1—C11—9C, 3S—5C—7C, 3S—11C—9C, 5C—3S—11C and 7C—9C—11C are found to be 119.8° [31] (calc. 120.5°), 127.0° (calc. 126.9°), 110.1° (calc. 110.4°), 113.2° (calc. 112.4°), 91.0° (calc. 91.0°) and 111.6° (cal. 112.1°), respectively. The optimized bond distances and bond angles are found to be compatible with the measured results. From TD-DFT calculations, the positive vibrational spectra, that is no any kind of imaginary frequency, are found that the optimized geometry is located at stationary point on the potential energy surface. The lowest vibrational harmonic frequencies for different solvents show that dichloromethane (DCM) is slighlty more stable than that of chloroform and chlorobenzene. Calculated first three vibrational harmonic frequencies for different solvent environment and the corresponding non-zero infrared intensities are given in Table 2. The geometrical optimization results reveal that the structure with minimum total energy is the C_1 form. All the 42 fundamental modes of vibrations were found to be IR and Raman active suggesting that the molecule possesses a non-centro symmetric structure. The visual comparison of the simulated IR and Raman spectra is shown in Figs. 2 and 3, respectively. As seen in Fig. 2, the compound exhibits the medium and huge peaks at 808 (symmetrical C–O—S stretching vibrations), 968 (C—C stretching band), 1456 (asymmetric CH_3 bending and C–OH bonds) and 1480 cm^{-1} (C–H, CH_2 and CH_3 bendings). As seen in Fig. 3, the compound shows the peaks at 1480 (thiophene) and 1592 cm^{-1} (asymmetric stretching mode vibrations of ionized carboxylic group).

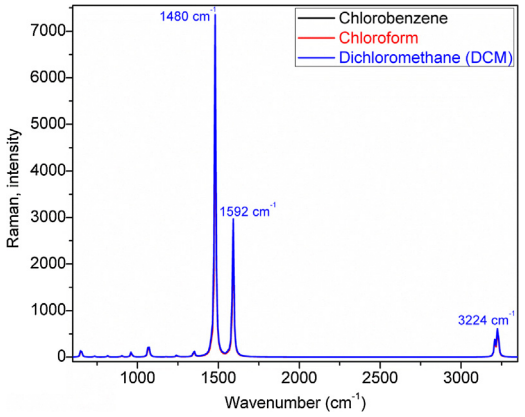

Fig. 3. Simulated Raman spectra for different solvents. (For interpretation of the references to colour in this figure legend, the reader is referred to the web version of this article.)

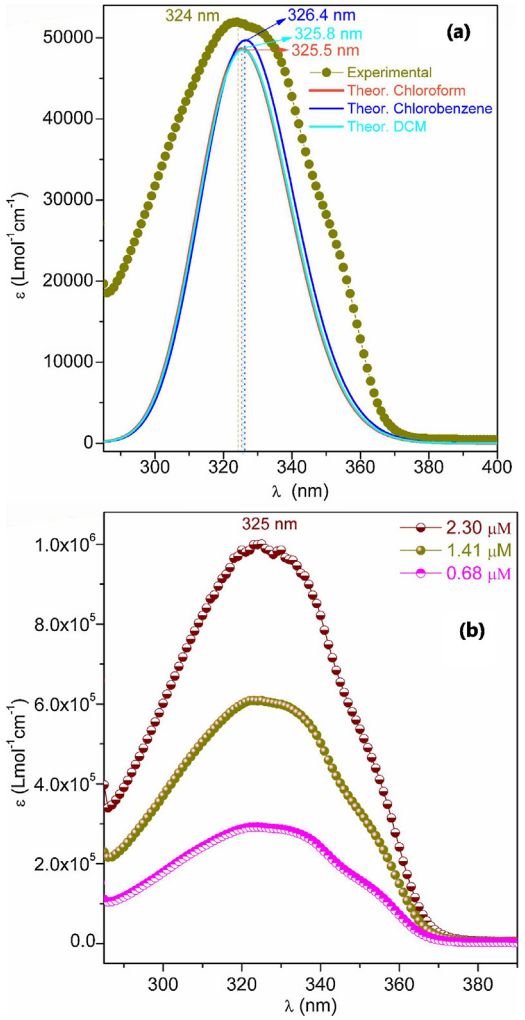

Fig. 4. The molar absorptivity plots vs. wavelength (λ) for (a) different solvents (experimental and theoretical) and (b) concentrations (experimental). (For interpretation of the references to colour in this figure legend, the reader is referred to the web version of this article.)

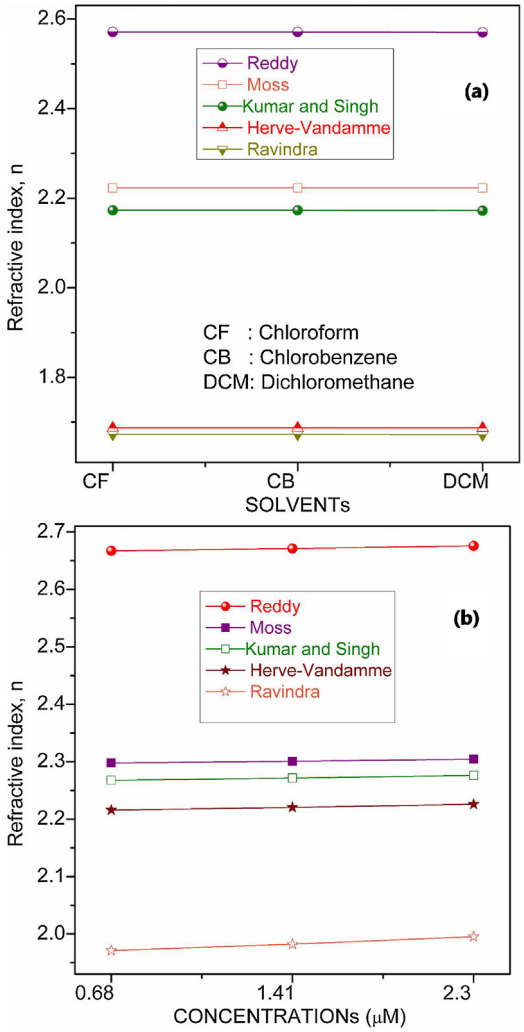

Fig. 5. The refractive index (n) curves of (a) different solvents obtained from DFT (b) 0.68, 1.41 and 2.30 μM obtained from experimental, Reddy, Moss, Kumar-Singh, Hervé-Vandamme and Ravindra relations. (For interpretation of the references to colour in this figure legend, the reader is referred to the web version of this article.)

4.2. Ultraviolet–visible spectroscopy

The molar extinction coefficient (ε), which is also known as the molar absorptivity and molar attenuation coefficient is an intrinsic property of the species. The ε can be given depends on the Beer-Lambert law [32],

$$\varepsilon = \frac{\text{Abs}}{\text{cL}} \tag{1}$$

where Abs is the absorbance, C is the concentration of a solution sample and L is the path length of the sample. The molar absorptivity value of the compound for chloroform solvent was experimentally obtained from Eq. (1). Fig. 5(a) indicates the molar absorptivity plots vs. wavelength (λ) obtained from experimental and theoretical results. As seen in Fig. 4(a), the material exhibits the maximum peaks of the molar extinction coefficients are found to be at 324 (experiment) and 325.5 (theory) nm for chloroform solvent. These results suggest that the experimental and theoretical molar extinction coefficients for all the related solvents exhibit one dominant peak in near ultraviolet region and experimental molar extinction coefficient values are compatible with theoretical ones. In addition, the maximum peak for chlorobenzene is found to be greater than that of chloroform and DCM.

Fig. 4(b) shows the absorbance curves of the compound solutions for different concentrations. The absorbance of the compound decreases with decreasing concentrations. The maximum peak position or wavelength for 0.68, 1.41 and 2.30 μm was found to be 325 nm. These results indicate that the concentration has significant effect on optoelectronic properties for the compound solution.

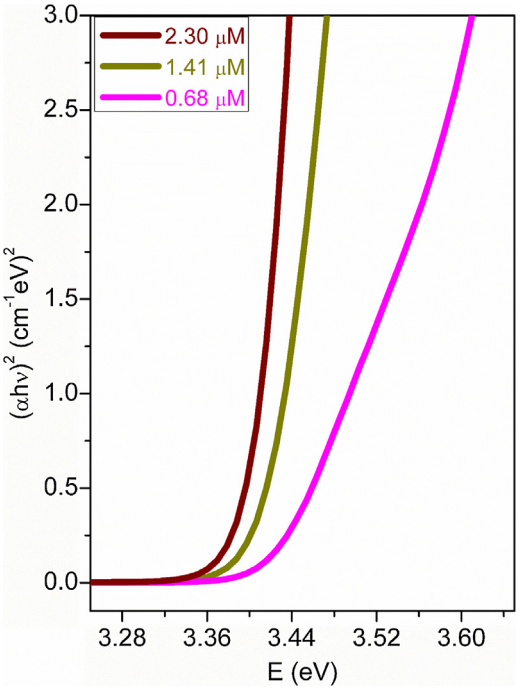

Fig. 6. The $(\alpha h\nu)^2$ vs photon energy of the title compound solutions for different concentrations. (For interpretation of the references to colour in this figure legend, the reader is referred to the web version of this article.)

4.3. The optical refractive index values (n)

To obtain the refractive index (n) values of the compound solved in different solvents, many equations such as Reddy, Ravindra, Kumar-Singh, Herve-Vandamme and Moss [33] were used together with the direct optical band gap $\left(E_{gd}\right)$ values. The n values for chloroform, chlorobenzene and DCM solvents (theoretical) and for chloroform solvent (experimental) were calculated by using the equations mentioned above. Fig. 5(a) indicates n curves vs. solvents obtained from DFT calculations for various relations. As seen in Fig. 5(a), the n values for chloroform and chlorobenzene are the same while the n values for DCM is slightly different. Similarly,n values obtained from Ravindra relation are the lowest, while the n values obtained from Reddy relation are the highest.

In addition, the direct refractive index (n_{gd}) values of the compound for 0.68, 1.41 and 2.30 μM were obtained by using the related equations mentioned above. Fig. 5(b) indicates the n_{gd} curves vs. concentrations for various relations. As seen in Fig. 5(b), the n_{gd} values for 2.30 μM are the highest, while the n_{gd} values for 0.68 μM are the lowest. On the other hand, the n_{gd} values obtained from Reddy relation are the highest, while the n_{gd} values obtained from Ravindra relation are the lowest. Obtained results suggest that the n_{gd} values increase with increasing concentration.

4.4. Electronic band structure

The energy gap which is HOMO–LUMO difference in energy, is an significant parameter in measuring the electron conductivity. Thus, HOMO and LUMO energies were obtained DFT and TD-DFT//B3LYP/6-331 G(d, p) level. The calculated energy value of HOMO is −5.6820, −5.6820, and −5.6841 eV for DFT and −6.0030, −6.0028 and −6.0012 eV for TD-DFT in chloroform, chlorobenzene and DCM solvents, respectively. Similarly, LUMO is −1.7937, −1.7932 and −1.7932 eV for DFT and −1.7524, −1.7540 and −1.7589 eV for TD-DFT in chloroform, chlorobenzene and DCM solvents, respectively. From HOMO–LUMO difference, we have obtained the E_g values from quantum chemical calculations. In addition, the measured results exhibit that from the linear region (the best fitting of results) of the variation of $(\alpha h\nu)^2$ versus E (hv) (see Fig. 6), the type of electron

Table 3
The experimental direct optical band gaps $\left(E_{gd},\ eV\right)$ and the absorption band edges $\left(E_{g-Abs}\right)$ depending on different solvents and concentrations (μM) and the energy gaps $(E_g,\ eV)$, obtained from DFT and TD-DFT calculations.

Solvents	E_{gd}	DFT	TD-DFT	Conc.	E_{gd}	E_{g-Abs}
Chloroform	3.361	3.888	4.250	**0.68**	3.408	3.307
Chlorobenzene	3.368	3.888	4.248	**1.41**	3.390	3.280
Dichloromethane	3.374	3.890	4.242	**2.30**	3.369	3.272

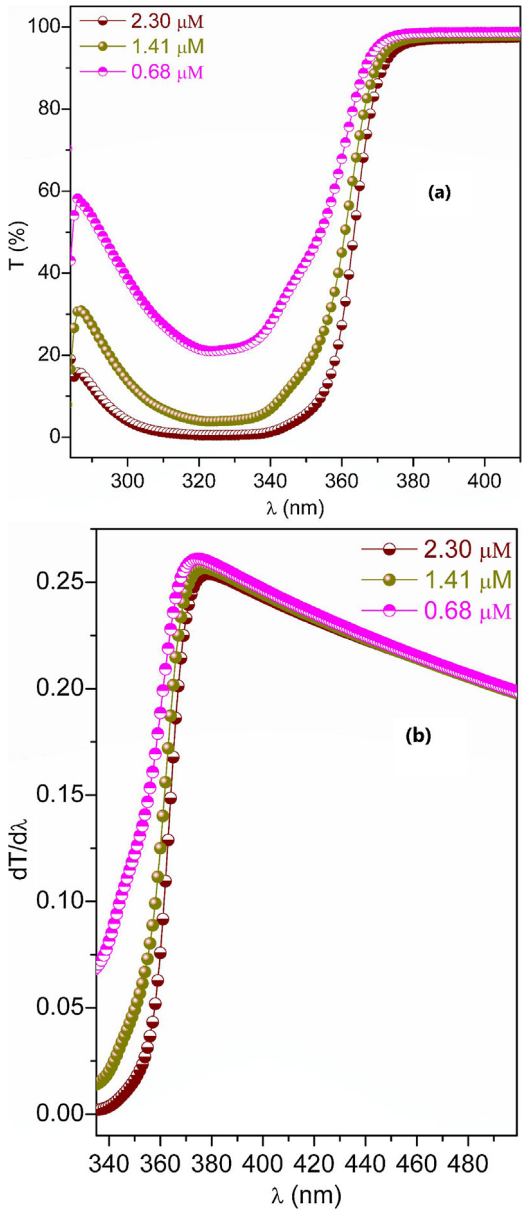

Fig. 7. (a) The transmittance (T) vs. λ (b) $dT/d\lambda$ plots vs. λ of the title compound solutions for different concentrations. (For interpretation of the references to colour in this figure legend, the reader is referred to the web version of this article.)

transition is direct allowed transition. The energy gap, E_g is determined by means of extrapolating the linear region of Fig. 6. Experimentally, several methods have been carried out to determine E_g values for different concentrations. The experimental direct optical band gaps E_{gd} depending on solvent and different concentrations obtained from DFT and TD-DFT calculations are tabulated in Table 3. As it is seen in Table 3, the energy gap for chloroform and chlorobenzene solvents gives reasonable values. For example, the measured E_{gd} for chloroform solvent is 3.361 eV, which is consistent with the theoretical E_g value (3.888 eV) obtained from DFT (see Table 3). From the results, one can conclude that chloroform solvent with the lowering of the band gaps can be preferred for optoelectronic applications or devices, which prefer lower band gaps because the electronic transfer is easier. It implies that the HOMO-LUMO energy gap for chloroform solvent compared to that of other solvent allows easy excitation of electrons from HOMO to LUMO.

The dispersion of the electronic bands for thicker the compound samples also increases due to interacting layers and thus reduces E_g as it seen in Table 3. We can also see that the band gap energies decrease with increment of the size of the materials at the nanoscale (see Table 3). This is the most remarkable feature of materials at nano level [34,35].

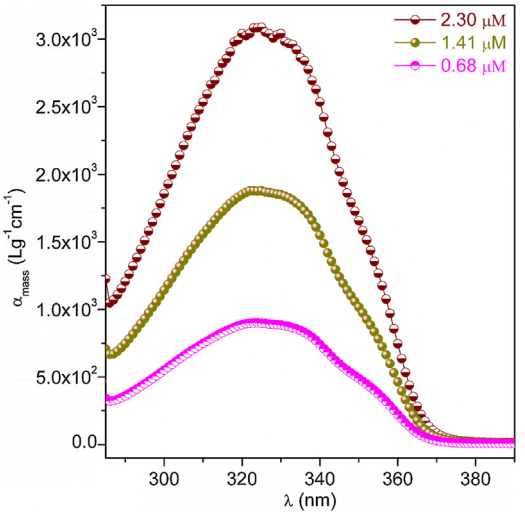

Fig. 8. The mass extinction coefficient (α_{mass}) plot vs. λ for different concentrations. (For interpretation of the references to colour in this figure legend, the reader is referred to the web version of this article.)

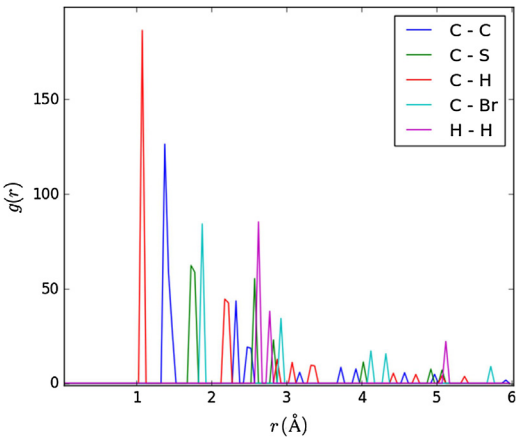

Fig. 9. Radial distribution functions (RDFs) of the carbon-carbon (C—C), carbon-sulphur (C–S), carbon-hydrogen (C–H), carbon-bromine (C—Br) and hydrogen-hydrogen (H—H) interactions. (For interpretation of the references to colour in this figure legend, the reader is referred to the web version of this article.)

4.5. *Experimental spectral behaviour of transmittance* (*T*)

The transmittance (*T*) spectra of the solutions of the compound for 0.68, 1.41 and 2.30 μM are shown in Fig. 7(a). *T* spectra of the compound for different concentrations exhibits minimum trenches at about 325 nm. After the minimum tendency of the wavelengths of *T*, a sharply increase is observed up to about 380 nm which is maximum constant value of the wavelengths.

The first derivative $\left(^{dT}/_{d\lambda}\right)$ of *T* versus λ are plotted to obtain the absorption band edge $\left(E_{g-Abs}\right)$ values for different concentrations as seen in Fig. 7(b). E_{g-Abs} values were obtained using the maximum peak position. E_{g-Abs} for different concentrations are tabulated in Table 3. As seen in Table 3, the E_{g-Abs} λ_{max} value decreases with decreasing concentration.

The α_{mass} values for different concentrations were calculated from Eq. (1). Fig. 8 shows α_{mass} plot vs. E of the compound. As seen in Fig. 9, the mass extinction coefficient varies significantly with photon energy. Obtained results indicate that α_{mass} values increase with the increment of concentrations.

4.6. *Mulliken atomic charge and dipole moment*

The Mulliken atomic charges (MACs) have a significant for quantum mechanical applications. MACs of the compound were gathered in Table 4. The charges of the same atoms in the different positions show different charge with each other for the atoms in the compound. The S3 atom exhibits a positive charge the value of MAC is bigger than others. Hydrogen atom exhibits a positive charge because it is an acceptor atom.

Table 4
Mullkien atomic charges (MACs) of the compound.

Atoms	MACs	Atoms	MACs
Br1	0.028901	C9	−0.027023
Br2	0.029072	C10	−0.027774
S3	0.363386	C11	−0.346973
S4	0.360134	C12	−0.345790
C5	−0.254684	H13	0.115808
C6	−0.250684	H14	0.116096
C7	−0.006593	H15	0.125485
C8	−0.004840	H16	0.125479

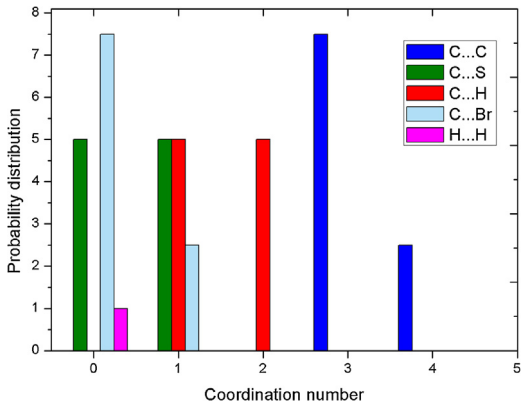

Fig. 10. Probability distributions of the carbon-carbon (C—C), carbon-sulphur (C–S), carbon-hydrogen (C–H), carbon-bromine (C—Br) and hydrogen-hydrogen (H—H) interactions. (For interpretation of the references to colour in this figure legend, the reader is referred to the web version of this article.)

The dipole moments are other important electronic properties. The bigger the dipole moment represents the stronger intermolecular interaction. The highest value of component of dipole moment along the y-axis (μ_y=2.2789 Debye) predicts large charge separation. The corresponding total dipole moment has been calculated to be 2.2796 Debye.

4.7. Radial distribution function and probability density

Fig. 9 shows the radial distribution functions (RDFs) analysis for carbon-carbon (C—C), carbon-sulfur (C–S), carbon-hydrogen (C–H), carbon-bromine (C—Br) and hydrogen- hydrogen (H—H) interactions of the compound. The RDFs are calculated for each atomic pairs. One can see that C–H has a narrower and higher distribution than the other pair interactions because of the weaker bond and the low atomic weight of the H atom. There also is a difference between the interactions. For C atoms, C–O is shorter than C—C, C–H, C–S and C–N interactions; for H, H—H is shorter than C–H. For all of the combinations, C–H has stronger interactions than the other ones. To study the influence of interactions of the atoms in the molecule, we also performed the probability distribution depending on the coordination number (see Fig. 10). The coordination number of C—C and C—Br interactions significantly decrease; for C–S and C–H interactions we have observed some fluctuations.

5. Conclusions

5,5′-Dibromo-2,2′-bithiophene organic compound has been searched using experimental technique and theoretical calculations. The results showed that the structure with minimum total energy is the C_1 form. Bond distances and angles are compatible available experimental results. The maximum peaks of experimental molar extinction coefficients for chloroform solvent and different concentrations are found to be compatible with theoretical value. The direct refractive index values oscillate based on increasing the concentration. The increase in concentration gives rise to the dispersion of the electronic bands thus decrease the band gap energies. Predicted band energy values for solvent are also agreement with the experimental data. The charges of the atoms in the different positions show different charge with each other for some carbon atoms. The larger dipole moment shows that the compound has the stronger intermolecular interaction. In addition, C–H interactions have a narrower and higher distribution.

Acknowledgments

The numerical calculations reported in this paper were partially performed at TUBITAK ULAKBIM, High Performance and Grid Computing Centre (TRUBA resources). This work was supported by the Ahi Evran University Scientific Research Projects Coordination Unit. Project Number: TBY.E2.17.008, Turkey.

References

[1] C. Xie, P. You, Z. Liu, L. Li, F. Yan, Light: Sci. Appl. 6 (2017) e1702.
[2] T. Hori, T. Masuda, N. Fukuoka, T. Hayashi, Y. Miyake, T. Kamikado, H. Yoshida, A. Fujii, Y. Shimizu, M. Ozaki, Org. Electron. 13 (2012) 335.
[3] S. Rajaram, R. Shivanna, S.K. Kandappa, K.S. Narayan, J. Phys. Chem. Lett. 3 (2012) 2405.
[4] A.D. Sio, C. Lienau, Phys. Chem. Chem. Phys. 19 (2017) 18813.
[5] M.Y. Ameen, T. Abhijith, D. Susmita, S.K. Ray, V.S. Reddy, Org. Electron. 14 (2013) 554.
[6] M. Neghabia, A. Behjata, Curr. Appl. Phys. 12 (2012) 597.
[7] F. Aziz, M.H. Sayyad, K. Sulaiman, B.Y. Mailis, K.S. Karimov, Z. Ahmad, G. Sugandi, Meas. Sci. Technol. 23 (2012) 014001.
[8] M. Murugavelu, P.K.M. Imran, K.R. Sankaran, S. Nagarajan, Mater. Sci. Semicond. Process. 16 (2013) 461.
[9] D. Liu, Y. Chu, X. Wu, J. Huang, Sci. China Mater. 60 (2017) 977.
[10] R.N. Gillanders, D.W. Ifor, G.A. Samuel, Turnbull, Sens. Actuators B: Chem. 245 (2017) 334.
[11] Y. Huang, R. Yuan, S. Zhou, J. Mater. Chem. 22 (2012) 883.
[12] Y. Huang, L. Fu, W. Zou, F. Zhang, N. J. Chem. 36 (2012) 1080.
[13] J.B. Wang, W.L. Li, B. Chu, C.S. Lee, Z.S. Su, G. Zhang, S.H. Wu, F. Yan, Org. Electron. 12 (2011) 34.
[14] S.D. Ogier, J. Veres, M. Zeidan, Application: WO Patent 2007082584 (2007).
[15] R. Hamilton, J. Smith, S. Ogier, M. Heeney, J.E. Anthony, I. McCulloch, J. Veres, D.D.C. Bradley, T.D. Anthopoulos, Adv. Mater. 21 (2009) 1166.
[16] T.K. An, S.-M. Park, S. Nam, J. Hwang, S.-J. Yoo, M.-J. Lee, et al., Sci. Adv. Mater. 5 (9) (2013) 1323.
[17] J. Zhang, G. Wu, C. He, D. Deng, Y. Li, J. Mater. Chem. 21 (11) (2011) 3768.
[18] C.A. Briehn, M.-S. Schiedel, E.M. Bonsen, W. Schumann, P. Angew Bauerle, Chem. Int. Ed. 40 (2001) 4680.
[19] A. Facchetti, M.H. Yoon, C.L. Stern, H.E. Katz, T.J. Angew Marks, Chem. Int. Ed. 42 (2003) 3900.
[20] T. Yamamoto, M. Arai, H. Kokubo, S. Sasaki, Macromolecules 36 (2003) 7986.
[21] Y.A. Getmanenko, S.-W. Kang, N. Shakya, C. Pokhrel, S.D. Bunge, S. Kumar, B.D. Ellmanb, R.J. Twieg, J. Mater. Chem. C 2 (2014) 256.
[22] C.-F. Chow, RCS Adv. 3 (2013) 18835.
[23] K. Kawashima, E. Miyazaki, M. Shimawaki, Y. Inoue, H. Mori, N. Takemura, I. Osaka, K. Takimiya, Polym. Chem. 4 (2013) 5224.
[24] Erika Bicciocchi, Ming Chen, Ezio Rizzardo, Kenneth P. Ghiggino, Polym. Chem. 4 (2013) 53.
[25] P.K. De, D.C. Neckers, Photochem. Photobiol. Sci. 12 (2013) 363.
[26] W. Kohn, L.J. Sham, Phys. Rev. 140 (1965) A1133.
[27] A.D. Becke, Phys. Rev. A 38 (1988) 3098.
[28] S.H. Vosko, L. Vilk, M. Nusair, Can. J. Phys. 58 (1980) 1200.
[29] C. Lee, W. Yang, R.G. Parr, Phys. Rev. B 37 (1988) 785.
[30] M.J. Frisch, G.W. Trucks, H.B. Schlegel, G.E. Scuseria, M.A. Robb, J.R. Cheeseman, G. Scalmani, V. Barone, B. Mennucci, G.A. Petersson, et al., Gaussian 09, Revision B.01, Gaussian, Inc., Wallingford, CT, 2009.
[31] G.J. Pyrka, Q. Fernando, Acta Cryst. C44 (1988) 562.
[32] A. Beer, Ann. Phys. 86 (1852) 78.
[33] S.K. Tripathy, Opt. Mater. 46 (2015) 240.
[34] M. Kurban, Ş. Erkoç, J. Comput. Theor. Nanosci. 12 (2015) 2605.
[35] M. Kurban, B. Gündüz, J. Mol. Struct. 1137 (2017) 403.